The EMBO Journal (2010) 29, 236–250 | © 2010 European Molecular Biology Organization | Some Rights Reserved 0261-4189/10
www.embojournal.org

THE EMBO JOURNAL

EMBO open

The PHCCEx domain of Tiam1/2 is a novel protein- and membrane-binding module

Shin-ichi Terawaki[1,2], Ken Kitano[1], Tomoyuki Mori[1], Yan Zhai[1], Yoshiki Higuchi[2], Norimichi Itoh[3], Takashi Watanabe[3], Kozo Kaibuchi[3] and Toshio Hakoshima[1,*]

[1]Structural Biology Laboratory, Nara Institute of Science and Technology, Takayama, Ikoma, Nara, Japan, [2]Department of Life Science, University of Hyogo, Kamigori-cho, Ako-gun, Hyogo, Japan and [3]Department of Cell Pharmacology, Graduate School of Medicine, Nagoya University, Nagoya, Aichi, Japan

Tiam1 and Tiam2 (Tiam1/2) are guanine nucleotide-exchange factors that possess the PH–CC–Ex (pleckstrin homology, coiled coil and extra) region that mediates binding to plasma membranes and signalling proteins in the activation of Rac GTPases. Crystal structures of the PH–CC–Ex regions revealed a single globular domain, PHCCEx domain, comprising a conventional PH subdomain associated with an antiparallel coiled coil of CC subdomain and a novel three-helical globular Ex subdomain. The PH subdomain resembles the β-spectrin PH domain, suggesting non-canonical phosphatidylinositol binding. Mutational and binding studies indicated that CC and Ex subdomains form a positively charged surface for protein binding. We identified two unique acidic sequence motifs in Tiam1/2-interacting proteins for binding to PHCCEx domain, Motif-I in CD44 and ephrinB's and the NMDA receptor, and Motif-II in Par3 and JIP2. Our results suggest the molecular basis by which the Tiam1/2 PHCCEx domain facilitates dual binding to membranes and signalling proteins.

The EMBO Journal (2010) **29,** 236–250. doi:10.1038/emboj.2009.323; Published online 5 November 2009
Subject Categories: signal transduction; structural biology
Keywords: CD44; GEF; GTPase; Par3; Rac

Introduction

T-lymphoma invasion and metastasis 1 (Tiam1) was originally isolated as an invasion-inducing gene product from T-lymphoma (Habets *et al*, 1994). Tiam1 belongs to the Dbl-family of guanine nucleotide-exchange factors (GEFs) that contain the Dbl-homology (DH) and Pleckstrin-homology (PH) tandem (DH–PH) domain, which directly catalyses the GDP/GTP exchange reaction in the GTPase cycle and thus facilitating the switch between inactive GDP-bound and active GTP-bound states (Mertens *et al*, 2003). The structures and functions of DH–PH domains have been extensively studied (Hakoshima *et al*, 2003; Rossman *et al*, 2005). Tiam1 acts as a GEF that specifically activates Rac GTPases to induce membrane ruffling and cell motility through reorganization of actin cytoskeletons and the establishment of cell polarity, which are believed to be processes closely related with cancer cell invasion and metastasis (Michiels *et al*, 1995). Crystallographic investigations have elucidated at atomic resolution the mechanism by which the Tiam1 DH–PH domain catalyses the GTP/GDP exchange of Rac1 (Worthylake *et al*, 2000).

Tiam1 has a closely related homolog Tiam2, also referred to as STEF (SIF and Tiam1 like-exchange factor), which was isolated by RT–PCR using mRNA extracted from mouse adult brain (Hoshino *et al*, 1999). SIF (still life) is a *Drosophila* Tiam1 homolog that has a function in the changes in morphology of axon terminals that occur with differentiation into mature synapses (Sone *et al*, 1997). All of these GEFs possess two PH domains, which are often referred to as PHn and PHc domains. The PHc domain is part of the well-characterized DH–PH tandem domain, whereas PHn is featured as part of a novel N-terminal PH–CC–Ex region that functions as a protein interaction module. This region is composed of three parts: a PH subdomain, a putative coiled-coil (CC) region and a conserved extra (Ex) region whose structural characteristics are undefined (Figure 1A). Stimulation of cells by treatment with serum resulted in membrane localization of these GEFs and subsequent induction of membrane ruffling (Michiels *et al*, 1997; Stam *et al*, 1997). This translocation from the cytoplasm to plasma membranes is an essential step for Rac activation. Interestingly, this PH–CC–Ex region, but not the PHn domain alone or the PHc domain of the DH–PH tandem domain, is essential for this process and has a crucial function in the redistribution of Tima1/2 in cells by interacting with plasma membranes (Michiels *et al*, 1997; Stam *et al*, 1997). Notwithstanding the extensive studies that have focused on this medically and biologically important GEF, the precise mechanism by which the PH–CC–Ex region contributes to membrane localization remains unknown.

The PH subdomain of the Tiam1/2 PH–CC–Ex region preferentially binds the products of phosphatidylinositol (PI)-3-kinase, PI-3,4,5-trisphosphate ($PI(3, 4, 5)P_3$) and PI-3,4-bisphosphate ($PI(3, 4)P_2$), as well as PI-4,5-bisphosphate ($PI(4, 5)P_2$) (Ceccarelli *et al*, 2007). More importantly, it has been suggested that the PH–CC–Ex region may function as a protein–protein interaction module. The region has been shown to directly bind to integral membrane proteins that contain the important cell adhesion molecule CD44, the

*Corresponding author. Structural Biology Laboratory, Nara Institute of Science and Technology, 8916-5 Takayama, Ikoma, Nara 630-0192, Japan. Tel.: +81 743 72 5570; Fax: +81 743 72 5579;
E-mail: hakosima@bs.naist.jp

Received: 13 May 2009; accepted: 8 October 2009; published online: 5 November 2009

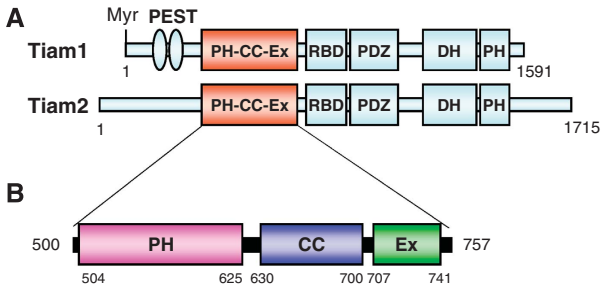

Figure 1 Domains in Tiam 1 and Tiam2. (**A**) Tiam1 and Tiam2 molecules possess five common domains/regions: the PH–CC–Ex region (orange), a Ras-binding domain (RBD), a PSD-95/DlgA/ZO-1 (PDZ) domain, a DH domain and the C-terminal PH (PHc) domain are indicated. The PH–CC–Ex region contains the N-terminal PH (PHn) domain. Two PEST sequences (ellipses) and the myristoylation site in Tiam1 are indicated. (**B**) Three subdomains of the Tiam2 PH–CC–Ex region used in this study.

hyaluronic acid (HA) receptor critical for cell motility and cell proliferation (Bourguignon *et al*, 2000), the axon guidance cue protein ephrin B1 that mediates neurite outgrowth (Tanaka *et al*, 2004), and the ephrin receptor Eph B2 (Tolias *et al*, 2007). Interacting with ephrins and Ephs, Tiam1 participates in the forward signalling of the Eph B receptor and the backward signal of ephrin B1. In addition to these membrane proteins, the PH–CC–Ex region has been reported to directly bind scaffolding proteins that bind Rac effectors such as JNK-interacting protein-1 and -2 (JIP-1 and JIP-2) (Buchsbaum *et al*, 2002), spinophillin/neurabin II (Buchsbaum *et al*, 2003) and Par3 of the Par3–Par6–aPKC complex (Chen and Macara, 2005; Nishimura *et al*, 2005). Moreover, Tiam1 has been found to form a complex with the Rac effector IRSp53 (insulin receptor substrate p53) by itself (Connolly *et al*, 2005). These findings suggest that some Rac GEFs can influence Rac GTPase signalling specificity in addition to promoting their activation (Buchsbaum *et al*, 2002).

Although biochemical studies have indicated a potential cooperative function of the PH subdomain and the extended CC and Ex segments of the Tiam1/2 PH–CC–Ex region for protein–protein interactions, the structural and functional roles of the extended regions remained elusive. Moreover, it was unclear whether the Tiam1/2-binding proteins possessed common structural and/or sequence characteristics. Here, we report the crystal structures of the PH–CC–Ex region of Tiam1 and Tiam2. The structures revealed that the three regions are combined into a unique globular structure, the PHCCEx domain, which creates a positively charged groove for binding to proteins along with the PI-binding site in the PH subdomain. Furthermore, we identified a negatively charged peptide region as the PHCCEx-binding site of CD44, which preserves the Motif-I sequence motif that is conserved in the PHCCEx-binding site of ephrin Bs. In Par3 and JIP2, we also identified another sequence motif, the acidic cluster Motif-II, for PHCCEx binding. Our results provide valuable clues towards understanding the molecular mechanism by which the PHCCEx domain mediates the Rac-specific GEFs to translocate towards plasma membranes through the dual recognition mode of PIs and membrane proteins, and also to recruit Rac effector proteins through binding to scaffolding proteins.

Results

Structural determination

The PH–CC–Ex regions of Tiam1 and Tiam2 display high sequence similarity (65% identity). The N-terminal boundary of the PH–CC–Ex regions was determined by comparison with other canonical PH domains, whereas the C-terminal domain boundary was not determined uniquely using sequences. Therefore, we prepared protein molecules that possessed different C-terminal ends for the crystallization. We first succeeded in crystallizing the Tiam1 PH–CC–Ex region, which comprised 274 residues (residues 429–702), although the crystals diffracted poorly ($\sim$4.5 Å resolution) (Terawaki *et al*, 2008). Crystals suitable for structure determination were obtained from a construct of the Tiam2 PH–CC–Ex region that included residues 500–757 (Figure 1B). Protein samples derived from the construct were crystallized into two different crystal forms, both of which contained four molecules per asymmetric unit. The structure of the initially obtained $P4_32_12$ crystals was determined using the multiwavelength anomalous dispersion (MAD) method combined with single isomorphous replacement using the native and selenomethione-substituted protein crystals, and subsequently refined using the $P2_1$ crystal to 2.1-Å resolution. The low-resolution structure of the Tiam1 PH–CC–Ex region was then determined by molecular replacement using the Tiam2 PH–CC–Ex structure as a search model and refined to 4.5-Å resolution.

The PH–CC–Ex region is folded into a single globular domain, PHCCEx domain

In our crystal structures, the PH–CC–Ex region is folded into a single globular domain (Figure 2A and B) that contains three-folded subdomains: an N-terminal PH subdomain (residues 504–625), a CC subdomain (residues 630–700) forming an antiparallel coiled coil with two long α-helices (α2 and α3) and a C-terminal Ex subdomain (residues 707–741) forming a small globular domain comprising three α-helices (α4–α6) (Figures 2C and 3). The PH and CC subdomains are positioned so as to form a V-shape, and the Ex subdomain is folded back to wedge into the gape of the V-shape. The resultant globular domain has overall dimensions of $35 \times 55 \times 70$ (Å), and a thickness of 30 Å. Thus, this PH–CC–Ex region is hereafter referred to as the PHCCEx domain. The compact globular domain structure is consistent with our sedimentation equilibrium data, which suggest a monomeric globular domain for the PH–CC–Ex region in solution with estimated molecular masses of 32.9 kDa (Tiam1) and 30.4 kDa (Tiam2) (Supplementary Figure S1).

In the asymmetric unit of the present crystal, the four PHCCEx domains essentially exhibit the same structure. Pairwise superposition on each subdomain indicates a small average root-mean-square (r.m.s.) deviation (0.3 Å) for both PH and Ex subdomains. The CC subdomain, however, displays a relatively large deviation (0.9 Å), which is associated with bending of a long CC structure and resulted in large average r.m.s. deviations (0.52–1.47 Å) for the overall PHCCEx domain (Supplementary Figure S2). The current structure contains no models for the loop between strands β3 and β4 (β3–β4 loop), which was poorly defined in the current electron density map.

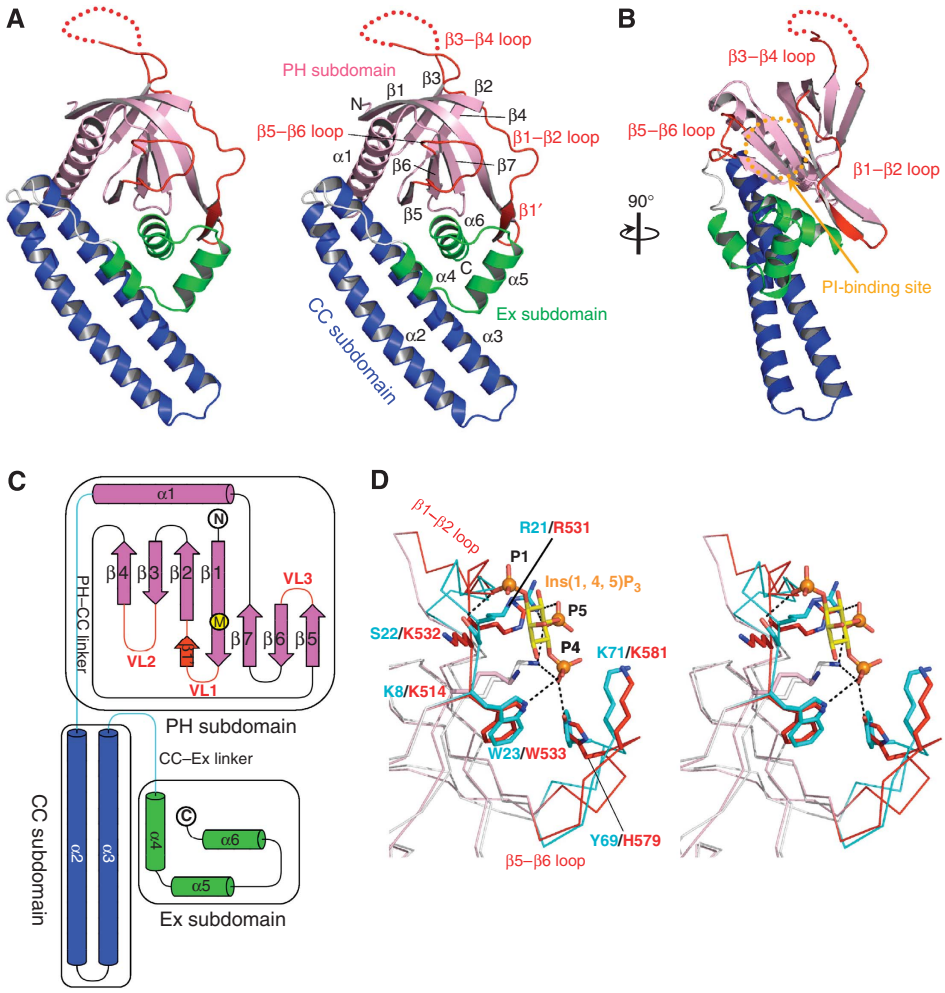

Figure 2 Structure of the Tiam2 PHCCEx domain. (**A**) A stereo view of the Tiam2 PHCCEx domain comprising three subdomains: the N-terminal PH subdomain (pink), a CC region (blue) and an Ex region (green) with three variable loops (red). Residues 553–560 (a dotted line) of loop β3–β4 are not defined in the current map. (**B**) As in (A) but with a rotation (90°) to show the putative PI-binding site. (**C**) Topology diagram of the Tiam2 PHCCEx domain. The missense mutation site (Ala441 of Tiam1) found in Tiam1 is marked by M. (**D**) The Tiam2 PH subdomain (pink and red) was superposed on the β-spectrin PH domain (grey and cyan) bound to Ins(1, 4, 5)P_3. Side chains important for direct interactions with Ins(1, 4, 5)P_3 are shown with the stick models with hydrogen bonds (dotted lines) between β-spectrin and Ins(1, 4, 5)P_3.

N-terminal PH subdomain

The PH subdomain of the Tiam2 PHCCEx domain comprises 122 residues and displays a typical PH domain fold, a β-sandwich capped at one end by a C-terminal α-helix (Figure 2C). At the β1–β2 loop, the PH subdomain forms an additional β1′ strand, which is located at the edge of the canonical seven-stranded β-sandwich and is associated with β1 strand. A DALI database search indicated the highest score for mouse β-spectrin PH domain (Hyvönen *et al*, 1995), which exhibits 30% sequence identity to the Tiam2 PH subdomain, with a small r.m.s. deviation (1.4 Å). On the other hand, low scores are obtained for phosphotyrosine-binding (PTB) domains with r.m.s. deviations larger than ∼3.2 Å. Similarly, poor structural similarity was observed with the EVH1/WH1 domain of Mena (Prehoda *et al*, 1999) and PHear domain of NECAP1 (Ritter *et al*, 2007). All of these domains possess peptide-binding sites for target proteins on the β-sandwich folds. It is well known that PTB domains possess a wide groove between β5 strand and α1 helix for peptide binding. In our PHCCEx domain structure, CC and Ex subdomains completely cover the corresponding groove of the PH subdomain. Like canonical PH domains, our PH subdomain possesses the narrow groove that seems not to accommodate a peptide chain. In fact, the isolated PH subdomain exhibited no CD44-binding activity (data not shown). Thus, it is unlikely that the peptide-binding ability is specially conferred by the PH subdomain of our PHCCEx domain.

Conventional PH domains, which were first identified as phosphoinositide-binding domains, have important functions in the spatial and temporal regulation of protein localization (Lemmon, 2008). The PI-binding affinities of PH domains were found to be dependent on three variable loops (β1–β2, β3–β4 and β6–β7 loops) that flank the open end of the β-sandwich (DiNitto and Lambright, 2006). The Tiam2 PH subdomain possesses a long β1–β2 loop similar to that of the β-spectrin PH domain and its closely related PH domains (Figure 2B). Indeed, structural comparison with the β-spectrin PH domain reveals that the Tiam2 PH subdomain exhibits similar conformations in terms of the β1–β2 and β5–β6 loops (Supplementary Figure S3A). For PI binding, β-spectrin

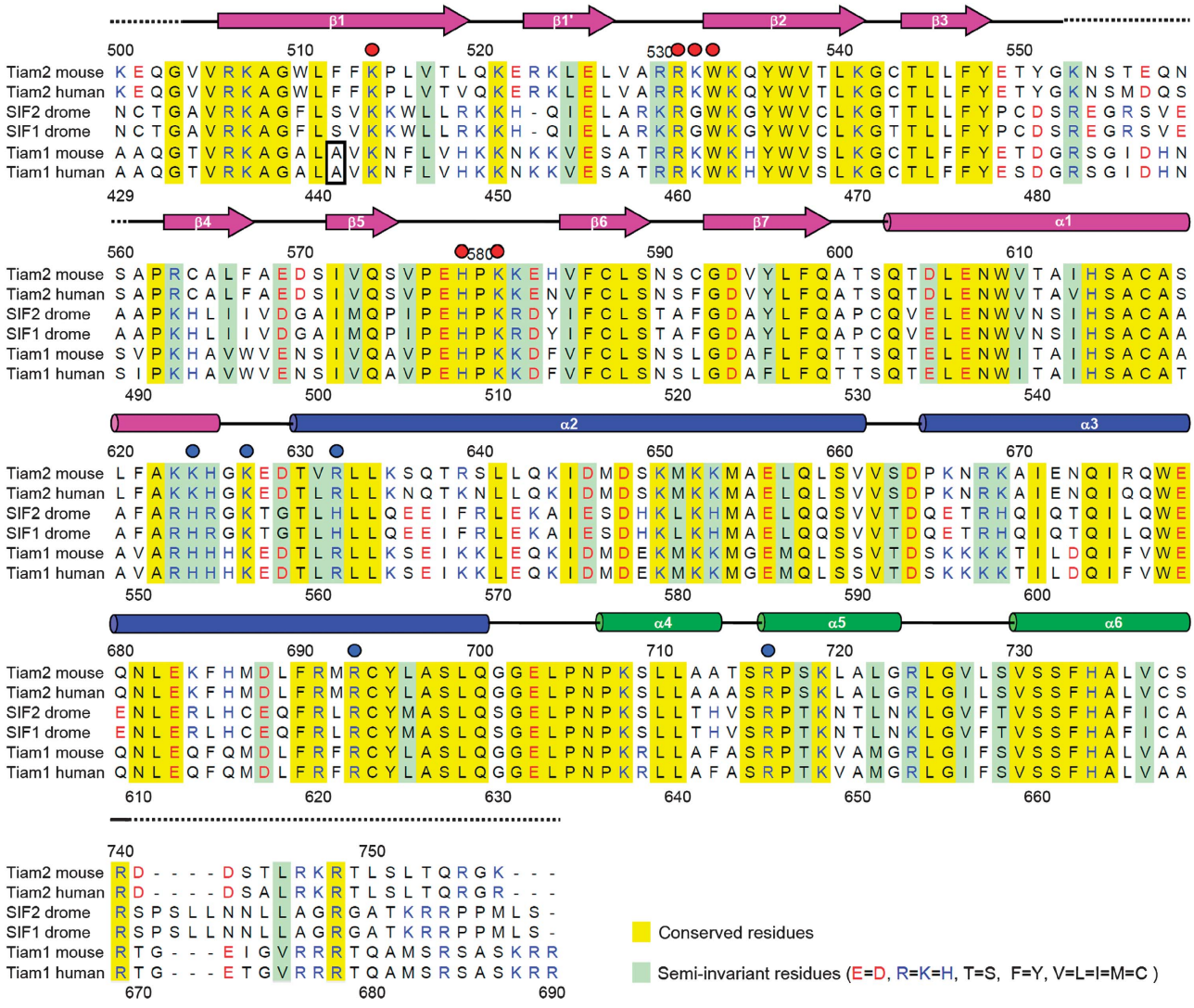

Figure 3 Sequence alignment of PHCCEx domains with secondary structure elements of the Tiam2 PHCCEx domain at the top. Conserved and semi-invariant (E = D, R = K = H, T = S, F = Y, V = L = I = M = C) residues are highlighted in yellow and blue-green, respectively. Acidic and basic residues are in red and blue, respectively. Residues predicted to be involved in interactions with phosphoinositides are indicated by red circles. Residues that were shown to be important for CD44 binding are indicated by blue circles. The Tiam1 missense mutation is indicated by a box.

and its closely related ArhGAP9 PH domains preserve two short sequences, K-X_n-R-S-W in β1–β2 loop and Y-*X*-K in β5–β6 loop (Hyvönen *et al*, 1995; Ceccarelli *et al*, 2007). These sequences are fairly well conserved in the Tiam1/2 PH subdomains. Overlay of Ins(1, 4, 5)P_3 bound to β-spectrin on the current structure suggests that similar PI binding could occur in the PH subdomain of the Tiam2 PHCCEx domain (Figure 2D).

Structural comparison with the Akt PH domain reveals conformational deviations in the β1–β2 and β5–β6 loops (Supplementary Figure S3B). In particular, loop β1–β2 of the Tiam1/2 PH subdomains lacks the K-X_n-K/R-*X*-R motif, which is characteristic in Akt, Btk and Grp1 PH domains that exhibit canonical PI binding with a high affinity using loops β1–β2 and β3–β4. Moreover, the β3–β4 loop of the Tiam2 PH subdomain displays profound conformational flexibility. These structural considerations support the earlier notion that the Tiam1/2 PH subdomain would use a non-canonical PI-binding mechanism like the case with β-spectrin (Rameh *et al*, 1997; Ceccarelli *et al*, 2007). In fact, like the ArhGAP9 PH domain, both the Tiam1 PH subdomain alone and the PHCCEx domain have been shown to exhibit strong preferences for PI(4, 5)P_2 as well as PI(3, 4, 5)P_3 and PI(3, 4)P_2 (Ceccarelli *et al*, 2007). This is in sharp contrast with the Akt PH domain, which exhibits a well-established preference for PI(3, 4, 5)P_3 and PI(3, 4)P_2 over PI(4, 5)P_2.

CC subdomain

The CC subdomain of the Tiam2 PHCCEx domain follows the C-terminal α1 helix of the PH subdomain through a four-residue linker (residues 626–629). Two long α-helices, α2 and α3, of the CC domain form extended antiparallel CC helices that are stabilized by being N-terminally capped by conserved Asp residues and C-terminally capped by main-chain amide groups of the following loops. In addition, α2 helix is C-terminally capped by Arg668 from α3 helix at the tip of the coiled coil. The antiparallel CC association is stabilized primarily by non-polar contacts involving the leucine

zipper-like motif (Supplementary Figure S4). At the C-terminal half of α2 helix, polar residues sparsely occupy the positions for leucine or non-polar residues of the heptad repeat and contribute towards stabilization of the coiled coil by polar contacts. These interactions include three hydrogen bonds (one between Asp648 and Asn681 at the centre of the coiled coil and two from Arg668 to carbonyl groups of Ser660 and Val662 at the tip of the coiled coil) and two salt bridges (one between Lys644 and Asp688 and the other between Lys652 and Glu679). These irregular interactions may confer a more flexible conformation of the CC subdomain compared with regular coiled coils such as the leucine zipper, which is stabilized by regular non-polar interactions between two intertwined helices.

Ex subdomain is folded into a novel small-helical domain

The CC subdomain is tethered to the Ex subdomain by a linker comprising six residues (residues 701–706). The compact fold of the Ex subdomain is achieved by close non-polar interactions of α6 helix with the groove formed by α4 and α5 helices (Supplementary Figure S5A). In addition to non-polar contacts, α6 helix is anchored to this groove by formation of a hydrogen bond between Arg740 of α6 helix and Ser718 of α5 helix. Three helices are N-terminally capped by Asn706 (α4 helix), Ser715 (α5) and Ser729 (α6). Moreover, α6 helix is C-terminally capped by Arg523 from β1' strand of the PH subdomain. The topology of the three helices is classified as a novel globular fold, an irregular array fold of short three-helices in the SCOP protein structure database (Murzin *et al*, 1995). This observation is consistent with its unique amino acid sequence, which exhibits no homology to any known helical domains such as the homeodomain, which consists of three short helices featuring the helix-turn-helix motif (Supplementary Figure S5B).

Inter-subdomain interactions in the PHCCEx domain

The globular assembly of the PHCCEx domain is constructed by direct interactions between each pair of the three subdomains. The interactions at each interface comprise a mixture of non-polar and polar contacts, including hydrogen bonds and salt bridges. The Ex subdomain is involved in close interactions with both the PH and CC subdomains, with a total buried accessible surface area of both interfaces of 2127 $Å^2$ (Figure 4A). At the interface with the PH subdomain, the Ex subdomain packs α5–α6 loop and α6 helix into the concave region of the PH subdomain formed by one β-sheet (β1′–β1–β7–β6–β5) of the β-sandwich. Three strands of the β-sheet (β1′, β1 and β7) predominantly make non-polar contacts with α5 and α6 helices of the Ex subdomain through conserved aliphatic residues (Figure 4B). In particular, β1′ strand is packed in the groove formed by α5 and α6 helices of the Ex subdomain and Leu525 is located deep inside the groove. In addition to non-polar contacts, Glu526 from β1′ strand forms a salt bridge with Arg724 from α5 helix (Ex). Thus, PH subdomain-specific β1′ strand has an important function in stabilization of the PH–Ex interactions. β5 and β6 strands make polar contacts with His734 and Ser731 from α6 helix through direct or water-mediated hydrogen bonds.

The Ex subdomain forms another groove comprising α4 and α6 helices, which accommodates the CC subdomain (Figure 4A). The middle region (Glu679-Phe690) of α3 helix of the CC subdomain is docked into this groove through the insertion of two projected non-polar residues, Met687 and Phe690 (Figure 4C). The interface between the Ex and CC subdomains, however, extends direct and water-mediated polar contacts including a salt bridge between Arg740 (α6) and Glu683 (α3).

The interface between the PH and CC subdomains is created primarily with α1 helix, β4–β5 loop and β5 strand of the PH subdomain, and makes contact with the tip of the CC subdomain (Figure 4A). The total buried accessible surface area of the PH–CC interface is 1237 $Å^2$, and contains hydrophobic contacts between non-polar side chains from α1 helix of the PH subdomain and both helices of the CC subdomain (Figure 4D). The interface contains two hydrogen bonds involving side chains and one salt bridge between Asp570 and Arg691.

Interaction between the PHCCEx domain and membrane proteins

We have outlined the PHCCEx domain structure above. Prior to efforts attempting to map the binding site on the PHCCEx structure, we tried to define the essential regions on membrane proteins for binding to the PHCCEx domain. CD44 was the first membrane protein identified that specifically binds to the Tiam1 PHCCEx domain (Bourguignon *et al*, 2000). The cytoplasmic tail of CD44 comprises 72 amino-acid residues (mouse residues 292–363) and has recently been characterized by spectroscopic and hydrodynamic methods (Mori *et al*, 2008). The study revealed that the cytoplasmic tail peptide adopts a random-coil structure in solution, which suggests that PHCCEx-CD44 binding may be mediated by protein–peptide rather than protein–protein interactions. Indeed, the N-terminal juxtamembrane region of the cytoplasmic tail contains a short peptide region (KKKLVIN at 300–306) responsible for binding to ezrin/radixin/moesin (ERM) proteins that acts as linker between plasma membranes and actin cytoskeletons (Mori *et al*, 2008). Besides the juxtamembrane region, the functional roles of the C-terminal long stretch are largely unknown. In an effort to define the peptide region of CD44 responsible for binding to the PHCCEx domain, we synthesized a series of N-terminal biotinylated CD44 tail peptides for surface plasmon resonance (SPR) measurements (Figure 5A and B). The Tiam2 PHCCEx domain did not bind the N-terminal CD44 peptide (residues 294–323) that contains the binding site for ERM proteins, but did bind the C-terminal peptides, which contain the acidic peptide comprising 14 residues (337–350). Next, we compared sequences of the PHCCEx-binding site of CD44s from different sources with the ephrin Bs cytoplasmic peptides. Interestingly, the sequence alignment reveals that CD44s conserve the acidic sequence motif, hereafter referred to as Motif-I, but also ephrin B's exhibit detectable homology to Motif-I (Figure 5C).

In our SPR measurements, the acidic peptide of CD44 comprising 24 residues (327–350) exhibited strongest binding to the Tiam2 PHCCEx domain with a dissociation constant K_D of 0.92 μM (Figure 6A). Similar results were obtained for the Tiam1 PHCCEx domain although the binding affinity is somewhat weaker than those of Tiam2. Moreover, our measurements showed that the acidic peptides of ephrin B1 and 2 indeed bind the Tiam2 PHCCEx domain with similar affinity (in the micromolar range) to that of CD44, whereas ephrin B3

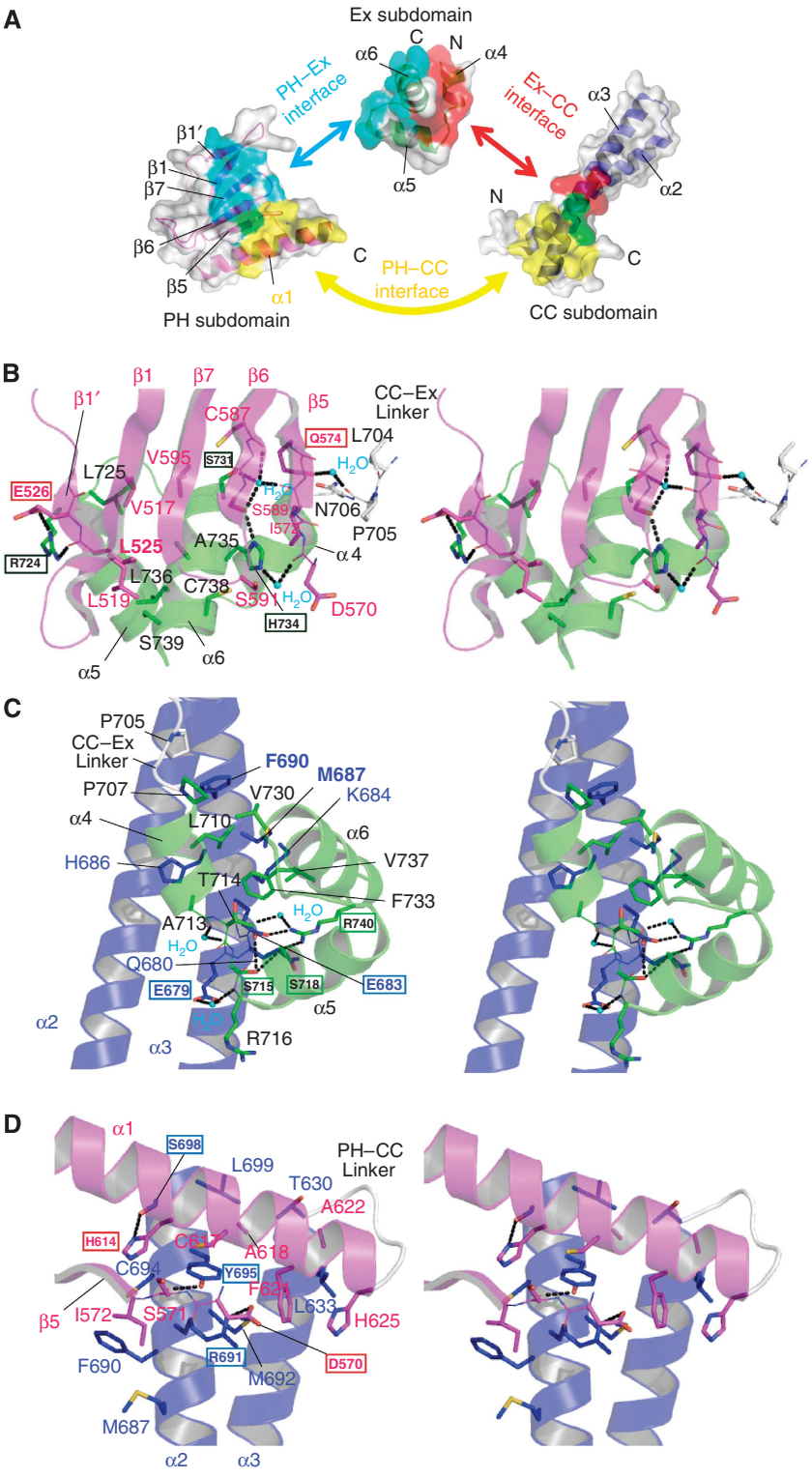

Figure 4 Inter-subdomain interactions. (**A**) Inter-subdomain interfaces are in blue (PH–Ex interfaces), yellow (PH–CC interfaces) and red (Ex–CC interfaces). The shared region for the two subdomains is in green. (**B**) A close-up view of the interface between the PH (red) and Ex (green) subdomains. Hydrogen bonds are indicated by broken lines. Residues whose side chains participate in polar interactions are labelled with boxes. (**C**) A close-up view of the interface between the CC (blue) and Ex (green) subdomains. (**D**) A close-up view of the interface between the PH (red) and CC (blue) subdomains.

exhibited weaker binding. At present, we presume that this may be caused by the insertion of residues GGG at the C-terminal half of the motif.

Mutational studies of the CD44 cytoplasmic peptide showed that two glutamates (Glu337 and Glu340) of the EPSE sequence and Cys345 of the CMTADE sequence are

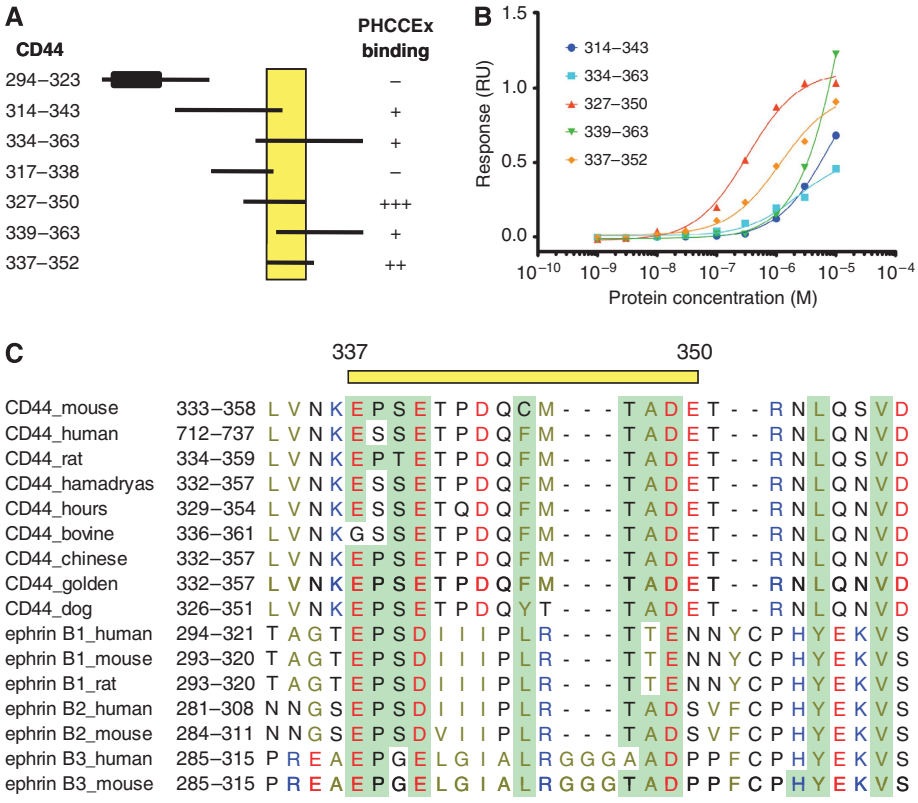

Figure 5 Interaction between the Tiam2 PHCCEx domain and CD44 cytoplasmic peptides. (**A**) Deletion mapping suggests 14 residues (337–350) of the CD44 cytoplasmic tail as the minimal-binding region as determined from the binding assay using SPR measurements. The yellow rectangle indicates the suggested minimum region. The bold rectangle indicates the ERM-binding region (residues 294–323) at the juxtamembrane region. (**B**) Interactions between the Tiam2 PHCCEx domain and the CD44 cytoplasmic peptides as determined from equilibrium SPR measurements. (**C**) Sequence alignment of PHCCEx-binding regions of CD44 and ephrin Bs using the program CLUSTALW. The suggested minimal region is indicated at the top. Invariant residues (E = D, T = S, C = L = F = Y) are highlighted in light green. Acidic and basic residues are in red and blue, respectively. Sequences are from the ExPASy database (human CD44: P16070, rat: P26051-2, mouse: P15379-2, hamadryas: P14745, horse: Q05078, bovine: Q29423, Chinese hamster: P20944, golden hamster: Q60522-2, dog: Q28284, human ephrin B1: P98172, mouse: P52795, rat: P52796, human ephrin B2: P52799, mouse: P52800, and human ephrin B3: Q15768, mouse: O35393.)

critical for binding to the Tiam2 PHCCEx domain (Figure 6B). This Cys position of mouse CD44 is conserved with a Phe residue in human and other mammalian CD44s and with a Leu residue in ephrin Bs. Thus, it is likely that hydrophobic residues at this mouse Cys position contribute to binding affinity by non-polar interactions with the PHCCEx domain.

Recently, Tiam1 has been shown to interact with the NR1 subunit of the NMDA-type glutamate receptor (NMDAR) (Tolias *et al*, 2005). Our SPR measurements showed that the Tiam1 PHCCEx domain strongly binds the NMDR loop I peptide (residues 591–610), but does not bind the C-terminal tail peptide (residues 921–938). Importantly, critical residues, two E's, L (for C) and S (for T), of the acidic motif are well conserved in the NMDAR loop I peptide (E**E**EEE**E**DALT**L**S**S**, where conserved residues are in bold with underlines) (Figure 6A).

Interaction between the PHCCEx domain and scaffolding proteins

Scaffolding proteins Par3 and JIP2, which have been shown to bind to the Tiam1/2 PHCCEx domain (Buchsbaum *et al*, 2002; Chen and Macara, 2005; Nishimura *et al*, 2005), lack peptide regions showing apparent homology to our proposed acidic motif, Motif-I, for PHCCEx binding. Earlier experiments have showed that part of the C-terminal CC region of rat Par3 was required for binding to the STEF/Tiam2 PHCCEx domain (Nishimura *et al*, 2005). This region of Par3 is conserved among various species and possesses the two characteristic regions comprising an N-terminal acidic cluster and a C-terminal basic region (Supplementary Figure S6A). We performed a pull-down assay using the GST-fused proteins of these regions and found that the Tiam2 PHCCEx domain binds to the N-terminal acidic cluster region of Par3, but not to the C-terminal basic region (Supplementary Figure S6B). Consistent with these results, the SPR measurements showed that the peptide comprising the acidic cluster region (mouse residues 931–960) binds the Tiam2 PHCCEx domain with a K_D value of 0.38 μM, which is comparable to that of CD44 (Figure 6A). This type of acidic cluster sequence can be found in the proposed PHCCEx-binding region (rat residues 434–522) of JIP2 (Buchsbaum *et al*, 2002) (Supplementary Figure S7), and our binding assay showed strong binding affinity to the acidic cluster of the mouse JIP2 peptide (residues 471–500) with a smaller K_D value of 0.11 μM (Figure 6A). Hereafter, we refer to these acidic clusters for PHCCEx binding as Motif-II, whereas the Par3 sequence does preserve some characteristic residues of the acidic motif Motif-I found in CD44 and ephrin Bs.

A

Peptide	Residues	Sequence	K_D (μM) Tiam2	Tiam1
Membrane protein				
CD44	327–350	SQEMVHLVNKEPSETPDQCM---TADE-	0.92 ± 0.02	1.23 ± 0.34
ephrin B1	294–312	-------AGTEPSDIIIPLR---TTENNY	1.58 ± 0.12	7.30 ± 0.84
ephrin B2	285–302	-------NGSEPSDVIIPLR---TADSVF	1.13 ± 0.07	6.11 ± 0.67
ephrin B3	286–303	-------REAEPGELGIALRGGGTAD	4.51 ± 0.29	10.9 ± 0.9
NMDAR	591–610	------VNSEEEEEDALTLS---SAMWFS	0.02 ± 0.001	0.17 ± 0.002
Scaffolding proteins				
Par3	931–960	-----KPMVDDDDEGMETLEED-TEESSRSGRESVS	0.38 ± 0.01	1.06 ± 0.21
JIP2	471–500	-----SEEEEEDEEEDEEDEED-AEDSVVPPGSRTT	0.11 ± 0.004	0.54 ± 0.02

B

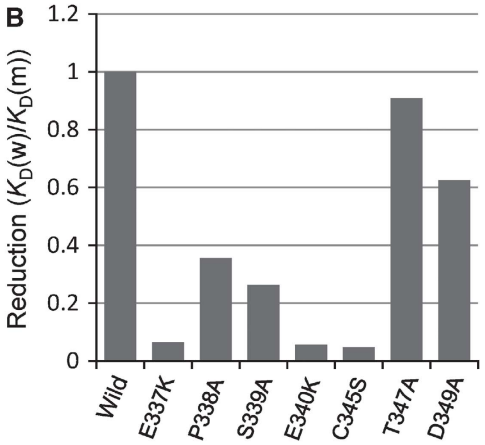

Figure 6 Interaction between the Tiam2 PHCCEx domain and peptides. (**A**) The obtained K_D values obtained from SPR measurements. The peptide sequences are aligned with basic (blue) and acidic (red) residues. Residues conserved among CD44s and ephrin Bs are in bold. Our mutation studies suggested CD44 residues (highlighted in yellow) critical for binding. (**B**) Binding assay of the Tiam1 PHCCEx domain to the mutant CD44 peptides. Reduction of binding affinity by mutation is represented in terms of the ratio of the observed K_D values of the mutated to the wild peptides.

Molecular surface properties

Consistent with the acidic peptide regions for Tiam1/2 binding, the electrostatic surface potential of the Tiam2 PHCCEx domain displays positively charged surfaces (Figure 7). A highly positively charged potential surface (the region enclosed by white broken lines in Figure 7A) corresponds to the putative PI-binding groove between β1–β2 and β5–β6 loops of the PH subdomain that has a width of ∼10 Å and includes conserved basic residues. In sharp contrast to this positive groove, the groove between β3–β4 and β5–β6 loops possesses negative charges (the region enclosed by red broken lines in Figure 7A), suggesting the absence of a PI-binding site in this region as discussed above. Interestingly, apart from the PI-binding site, the second region possessing highly positive charges expands from the Ex to CC subdomains (the region with yellow broken lines in Figure 7A) and extends to the side wall of the domain towards the bottom side (Figure 7B). This positively charged surface contains clusters of conserved basic residues (Figure 7C). There is no such positively charged large surface on the other side wall (Figure 7D).

Peptide-binding site of the PHCCEx domain

Next, we attempted to determine the CD44-binding surface on the PHCCEx domain. As the Tiam2 PHCCEx domain binds acidic peptides, we supposed that a basic region on the PHCCEx domain should be responsible for peptide binding. Eight point mutant proteins were generated and purified in which each conserved basic amino-acid residue was replaced with alanine, and these were subjected to SPR measurements with the 24-residue CD44 peptide (Figure 8A). Compared with the wild-type protein, five alanine mutants (Lys627, Lys624, Arg632, Arg716 and Arg693) comprising residue changes located at the second positively charged region displayed a reduction in binding affinity to the CD44 peptide (Figure 8B). In contrast, three alanine mutants (Lys650, Lys653 and Arg691) did not show any detectable reduction in binding affinity: the first two mutants comprised residue changes located at the middle of α2, which is outside of the second positively charged region and the third mutant (Arg691) comprised a residue change located at α3 faces on the opposite side of the surface. Similar results were obtained for the Par3 peptide (Supplementary Figure S8). The most significant reduction in binding to the CD44 peptide was observed for the alanine mutant Arg716, which comprised a residue change located in the Ex subdomain and is facing towards the same molecular surface as that used for PI binding of the PH subdomain, that is, the proposed molecular surface facing plasma membranes. The second was the alanine mutant Arg693, which comprised a residue change located at the centre of the positively charged region (Figure 8A). Compared with the wild-type PHCCEx domain, the single (R716A) and the double (R693A and R716A) mutations display 5- and 24-fold decreases of CD44-binding affinity in terms of K_D values, respectively (Figure 8C). Compared with CD44, these mutations display smaller (∼2- and ∼3-fold) decreases of Par3-binding affinity, respectively. These results indicated that residues in the second positively charged region expanding the Ex and CC subdomains have an

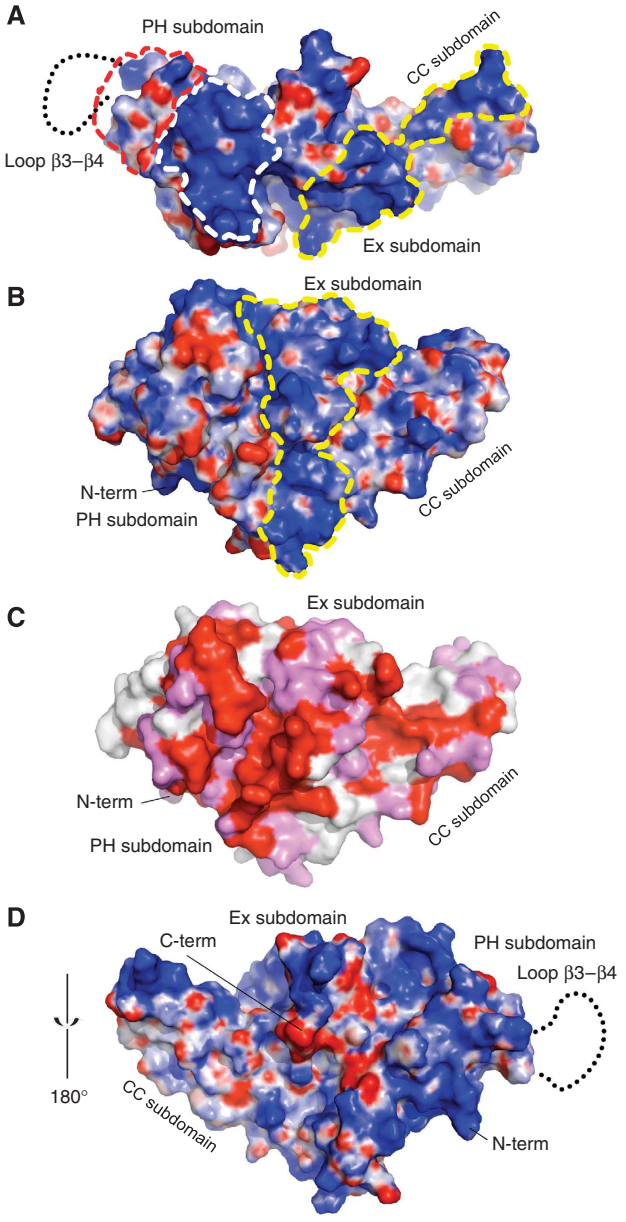

Figure 7 Molecular surface property of the Tiam2 PHCCEx domain. (**A**) A top view of surface electrostatic potentials of the PI-binding surface. Positive (blue: +10 kT/e) and negative (red: −10 kT/e) potentials are mapped on the van der Waals surface. On the PH subdomain, the highly positively charged potential region including basic residues (Lys514, Lys531, Arg530, Lys532, Lys534, Lys581 and Lys582) for PI binding is circled with white broken lines. The second positively charged region is circled with yellow broken lines (see text). (**B**) A side view of surface electron potentials. The second positively charged region is circled with yellow broken lines (see text). (**C**) Conserved residues in Tiam1 and Tiam2 from different sources are mapped on the molecular surface viewed from the same direction as in (B), with identical (orange), related (purple) and non-conserved (white) residues. (**D**) As in (B) but with rotation around a vertical axis of 180°.

important function in interactions with the acidic motif and acidic cluster of Tiam1/2-binding proteins.

Mutations that reduce CD44- and Par3-binding affinity do not affect on PI(3, 4, 5)P_3-binding affinity (Supplementary Figure S9A), implying that the PHCCEx domain binds PIs and proteins with no significant interference or cooperativity. Indeed, PI(3, 4, 5)P_3 binding does not significantly affect on CD44-, Par3- and ephrin B1 bindings (Supplementary Figure S9C). Similarly, these peptide bindings do not affect on PI(3, 4, 5)P_3 binding to the PHCCEx domain (Supplementary Figure S9D). Taken together, we propose simultaneous binding of the PHCCEx domain to both PIs and the acidic peptide region of signalling proteins (Figure 8D).

The peptide binding by the PHCCEx domain in vivo

With a set of Tiam1 mutants, we addressed whether the identified interaction site is relevant to the protein interactions within cells. The interaction of HA-tagged full-length Tiam1 with GFP-tagged full-length Par3 was tested by immunoprecipitation assay from coexpressed COS7 cell lysates (Figure 9A). The wild type of Tiam1 coprecipitated with GFP-Par3. We used Tiam1 with a double mutation (R622A and R645A) on the peptide-binding site of the PHCCEx domain, corresponding to the Tiam2 double mutation (R693A and R716A). We found that the double mutation reduced Par3 binding to ∼65%, suggesting that the identified binding site has a function in *in vivo* interactions with Par3.

To clarify the functional significance of the binding site, the dominant negative effects of the isolated PHCCEx domain on lamellipodia formation was estimated. The isolated Tiam1/2-binding region of Par-3 (the rat 4N/1 fragment, residues 937–1038) has been shown to be sufficient to increase the amount of Rac1-GTP for induction of lamellipodia by binding to Tiam1 (Nishimura *et al*, 2005). Contrary to this activation, the isolated Tiam1 PHCCEx domain was known to be a dominant-negative factor that interferes with Par-3-Tiam1 binding (Matsuo *et al*, 2002; Nishimura *et al*, 2005). In the absence of the PHCCEx domain, the Par3 4N/1-mediated increase in lamellipodia formation was observed. This Par3 4N/1-mediated increase was significantly suppressed by co-expression of the wild-type PHCCEx domain, which could interfere with Par3-Tiam1 binding, whereas the suppression was weakened by each single mutation (R622A or R645A) on the PHCCEx domain (Figure 9B). The suppression was further alleviated by the double mutation (R622A and R645A). Together with the coimmunoprecipitation experiments, we concluded that Par3 binding to the positively charged peptide-binding site of the Tiam1 PHCCEx domain has a critical function in lamellipodia formation induced by Tiam1-madiated Rac activation in cells.

Discussion

PI binding and peptide binding for membrane recruitment

The Tiam1/2 PHCCEx domains are essential for the interaction with plasma membranes and the induction of ruffling meditated by Rac activation (Michiels *et al*, 1997; Stam *et al*, 1997). Deletion of the CC or Ex regions also abolished membrane localization of Tiam1 and membrane ruffling (Stam *et al*, 1997), suggesting that both the PH subdomain and the extended CC–Ex region are necessary for effective association with plasma membranes. The PHCCEx domain has been shown to display four-fold stronger overall affinity for PI's as compared with the isolated PH subdomain (Ceccarelli *et al*, 2007). These differences may be caused by wider positively charged surfaces of the PHCCEx domain

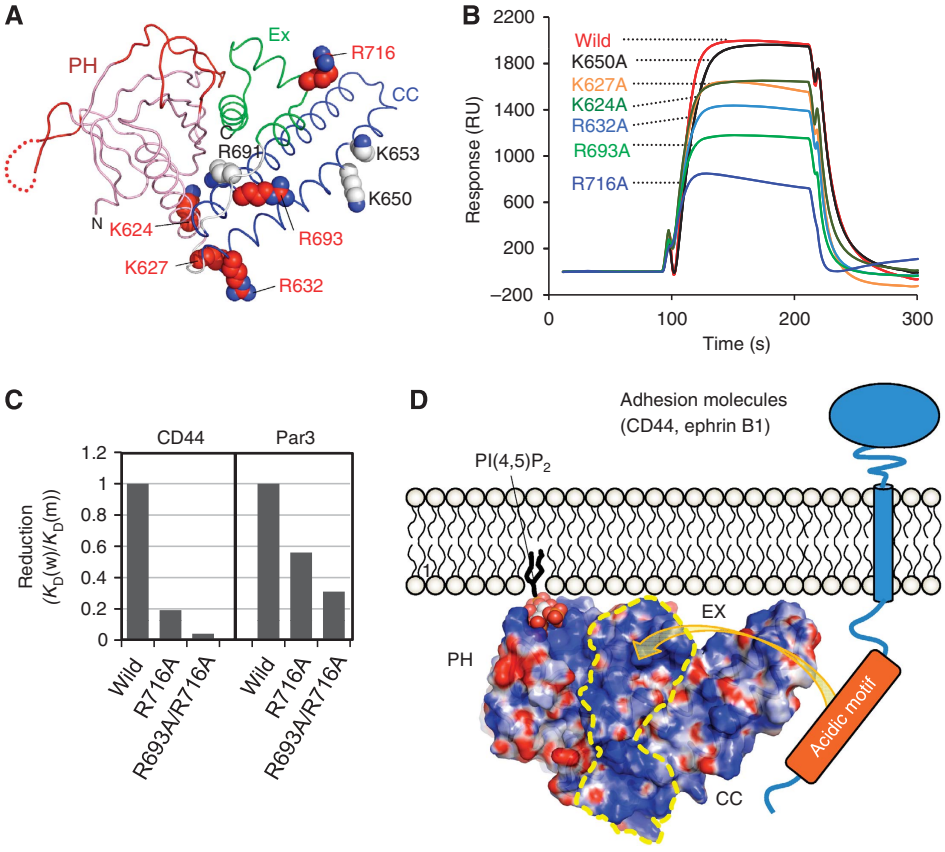

Figure 8 CD44 binding surface of the Tiam2 PHCCEx domain. (**A**) Mutated residues are mapped on the Tiam2 PHCCEx domain structure. Residues with detectable effects on CD44 binding are shown in red and residues with no effect on CD44 binding are shown in grey. (**B**) Sensor diagrams obtained from SPR measurements with the CD44 peptide (residues 327–350) immobilized on a sensor chip with injection of mutated Tiam2 PHCCEx domains (1 μM). (**C**) Mutation effects on K_D values. Effects on CD44- and Par3-binding affinity by mutations were estimated in terms of K_D values determined by SPR measurements. (**D**) Model of membrane targeting by the PHCCEx domain. PI(4, 5)P_2 is docked into the PH subdomain. Transmembrane proteins such as CD44 and ephrin B1 possess a unique acidic motif (orange) for binding to the PHCCEx domain.

than that of the PH subdomain alone. Moreover, the CC–Ex region may contribute to stabilize the PH subdomain structure for its full affinity for PI's. The PH subdomain cannot be functionally exchanged with other PH domains (Michiels *et al*, 1997), in part due to a lack of binding surfaces to the CC and Ex subdomains on the other canonical PH domains. Comparing with Tiam1, the Tiam2 PHCCEx domain exhibited ~2-fold increased PI(3, 4, 5)P_3-bind affinity (Supplementary Figure S9A and B). This small but detectably stronger binding affinity seems to be consistent with its higher affinity to CD44 and other proteins than that of Tiam1 as mentioned above (Figure 6A). We speculate that binding to PI's through the PH subdomain mediates membrane localization and subsequent binding to membrane proteins through the CC–Ex subdomain enhances localization at restricted areas on the plasma membrane to accomplish the proper induction of membrane ruffling. Genome-wide biochemical analysis of the PH domains suggests that binding of PIs by the PH domains is not always sufficient to define the specific cellular localization (Lemmon, 2008). The specific cellular localization through the PH domains should be defined by an interaction with secondary-binding partners (Levine and Munro, 2002; Godi *et al*, 2004; Zhao *et al*, 2007). This consideration is in line with our structures, which reveal that the PHCCEx domain mediates both processes.

Peptide-binding modes

The acidic motif (Motif-I) and the acidic cluster (Motif-II) provide no common sequence. Differences in both the binding motifs and the binding affinities may suggest that the binding modes differ somewhat between membrane and scaffold proteins, although further experiments are needed to clarify this point. The PHCCEx-binding motifs found in this study are distinct from the binding motifs of known protein interaction domains besides the PH domain of IRS-1 and -2 (Burks *et al*, 1998), which binds acidic peptides that may be similar to the acidic clusters of Par3 and JIP2 for PHCCEx binding. However, the homology between the PH subdomain of the Tiam1/2 PHCCEx domain and the IRS-1/2 PH domain is poor (13% identity). Small GTPase Ran possesses an acidic sequence at the C-terminal tail that facilitates protein–protein interactions (Vetter *et al*, 1999). We detected significant binding between the Tiam1 PHCCEx domain and the Ran acidic tail peptide (residues 146–216) that contains the DPEDDL motif (Supplementary Figure S10). The observed interaction may have a function in Tiam1 functions in the nucleus where Ran is predominantly located.

Dual binding to Tiam1 and ERM proteins

CD44 is a member of the family of adhesion molecules that is linked to actin cytoskeletons, an interaction that is mediated

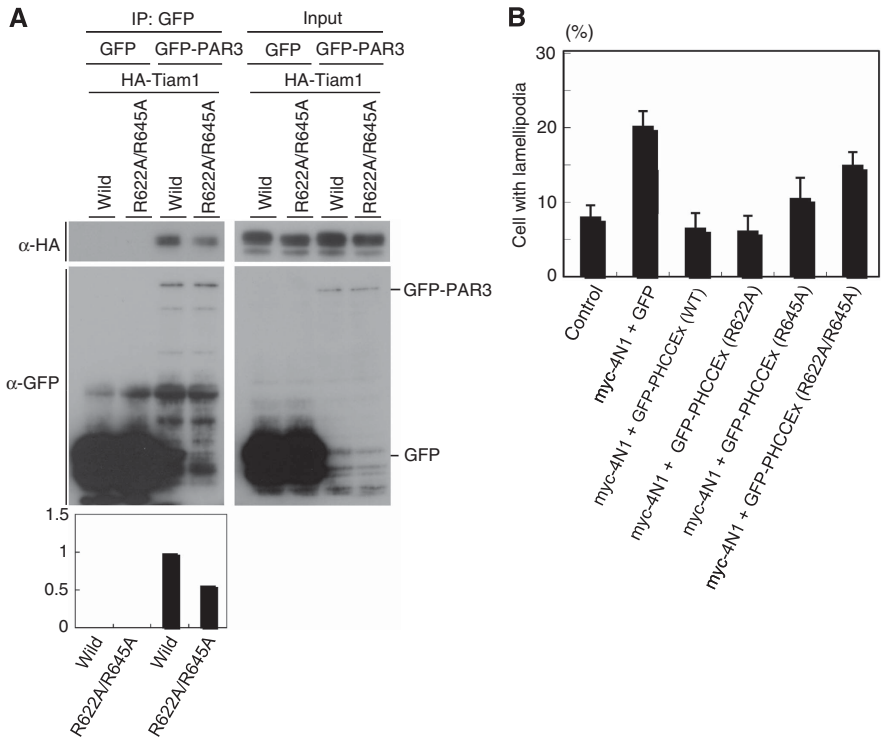

Figure 9 The Tiam1 PHCCEx domain functions in cells. (**A**) Coimmunoprecipitation of Tiam1 and Par-3 in cells. COS7 cells lysates expressing indicated proteins, HA-Tiam1 and GFP-Par3 or control GFP, were incubated with anti-GFP antibody. The immunoprecipitates were analysed by immunoblotting with the indicated antibodies. The relative ratio of Tiam1 to immunoprecipitated GFP-Par-3 is shown at the bottom. (**B**) GFP-positive cells were scored by the presence of lamellipodia. Inhibition of the Par-3 4N/1-mediated Rac1 activation by the wild-type and mutant Tiam1 PHCCEx domains was estimated.

by specific binding between the cytoplasmic tail of adhesion molecules and the N-terminal FERM domain of ERM proteins (Yonemura *et al*, 1998). The mechanism by which the FERM domain recognizes peptides of signalling proteins has been clarified by investigation of the crystal structures of the radixin FERM domain bound to ICAM-2, PSGL-1, CD43, NEP or CD44 (Hamada *et al*, 2000, 2003; Takai *et al*, 2007, 2008; Terawaki *et al*, 2007; Mori *et al*, 2008). All of these structures show that ERM proteins bind both plasma membranes and the juxtamembrane regions of the cytoplasmic tails through the FERM domain. Tiam1/2 also binds plasma membranes, but specifically to off-membrane peptide regions of cytoplasmic tails. The PHCCEx-binding sites of CD44 and ephrin B1 are located at positions 46 and 39 residues, respectively, off the transmembrane helix embedded in the plasma membrane. In the case of CD44, the PHCCEx-binding site is 30 residues from the FERM-binding site at the juxtamembrane region. As our hydrodynamic studies suggest that the cytoplasmic tail adopts a flexible random-coil state in solution (Mori *et al*, 2008), we speculate that Tima1/2 and ERM proteins may independently bind CD44. Our binding assay showed that the radixin FERM domain binds the sensor chip that is coupled with the Tiam2 PHCCEx domain in the presence of the CD44 cytoplasmic tail (Supplementary Figure S11), suggesting formation of the ternary complex of the radixin FERM domain, the CD44 cytoplasmic tail and the Tiam2 PHCCEx domain.

PHCCEx-mediated specificity

Given that Tiam1/2 are integrated in different signalling pathways at the membrane (Minard *et al*, 2004; Marinissen and Gutkind, 2005), what dictates the selection of proteins to which Tiam1/2 bind in response to extracellular stimuli is an interesting question. Both Tiam1 and Tiam2 are highly expressed in brain (Habets *et al*, 1994; Matsuo *et al*, 2002) and have important functions in neurite outgrowth and the development and remodelling of synaptic connections by specific binding to the acidic motifs of ephrin Bs and NMDAR colocalized with EphB2 (Tanaka *et al*, 2004; Tolias *et al*, 2005; Tolias *et al*, 2007). Tiam1/2 also participate in establishing cell polarity and promoting cell migration in other cells such as epithelial cells, fibroblasts, T-lymphoma and other tumour cells as well as neurons. For these functions, Par3 is an important protein that activates Tiam1 to induce lamellipodia by Rac activation. In general, GEF-binding scaffolding proteins govern the selection of signal outputs (Marinissen and Gutkind, 2005). For example, Tiam1 bound to JIP2 leads to the selective stimulation of p38 on Rac activation through JIP2 binding to MLK3, MLK7 and p38 kinase. Other scaffolding proteins, spinophilin and IRSp53, also contribute to the selection of downstream proteins, p70 S6 kinase and WAVE2, respectively, although the binding sites of these proteins are unidentified yet (Buchsbaum *et al*, 2003; Connolly *et al*, 2005). In metastatic breast tumour cells, Tiam1 binding to CD44 is believed to promote cytoskeleton-mediated tumour cell migration during breast cancer progression (Bourguignon *et al*, 2000).

PHCCEx domain family and medicine

In humans, there are 69 distinct members of the Dbl-family GEFs (Rossman *et al*, 2005). Besides Tima1/2, RasGRF1/2, Fabin, Fgd1/2, Farp1/2 and BAC85128 possess an extra PH

domain in addition to the DH–PH tandem domain. RasGRF1/2 is a Ras-specific GEF known to possess a PHCCEx-like domain, in which the Ex subdomain is substituted with an IQ motif, and binds JIP2 as well as Tiam1 (Buchsbaum *et al*, 2002). The other member, however, possess no apparent CC and Ex subdomains following the extra PH domain. Some GEFs, such as Lbc for RhoA, p115-RhoGEF and AAH42606, seem to possess the DH–PH domain followed by potential CC regions, although further experiments are needed to determine whether the domain and the following region organize to form a unified functional domain.

Tiam1 was shown to be associated with malignant transformation of cancer cells (Michiels *et al*, 1995). Tiam1-deficient mice displayed significantly fewer and smaller tumours compared with wild-type mice (Malliri *et al*, 2002). Moreover, Tiam1 expression in human tumour cell lines and carcinomas has been reported (Bourguignon *et al*, 2000; Minard *et al*, 2004; Liu *et al*, 2005, 2007; Adithi *et al*, 2006; Malliri *et al*, 2006). These reports suggest that Tiam1 should have a critical function in the progression of epithelial cancers. Interestingly, a missense mutation (Ala441Gly) in the N-terminal PH subdomain of Tiam1 was identified from tumours and cell lines of renal cell carcinoma (Engers *et al*, 2000) (Figures 2C and 3). This residue is located at a position where non-polar contacts are made with a Trp residue (Trp462 of Tiam1 and Trp533 of Tiam2) that directly binds PIs, whereas our PI-binding assay showed that the mutation induces no significant changes in the binding affinity to PI(3, 4, 5)P_3 (Supplementary Figure S9B). Thus, the mechanism by which the mutation generates a dominant active phenotype is currently unknown.

In summary, we have demonstrated the structural basis for the unique ability of the PHCCEx domain to activate Tiam1/2. The specific interface identified here delineates the molecular interaction of Tiam1/2 with CD44, ephrin Bs, JIP2, Par3 and NMDAR, and provides a target for the design of therapeutics aimed at disrupting Rac activation in processes involving proteins in cell–ECM and cell–cell adhesion, cell signalling and the establishment of cell polarity. Finally, we provide a structural template for mutational studies directed towards defining the biological role of Tiam1/2 in activating Rac in cells and, ultimately, in whole animals. The next challenge will be to determine the precise mechanisms involved in the recognition of signalling proteins by the PHCCEx domain, and the relationship between the GEF activity of recruited Tiam1/2 and functions of the signalling proteins.

Materials and methods

Sample preparation

The PH–CC–Ex regions of mouse Tiam1 (residues 429–702) and Tiam2 (residues 500–757) were expressed in *Escherichia coli* cells, purified and crystallized as described earlier (Terawaki *et al*, 2008). The mutants were constructed using QuickChange (Stratagene) and confirmed by DNA sequencing. For MAD experiments, the selenomethionine (Se-Met)-substituted protein was expressed using the technique based on the inhibition of methionine biosynthesis (Duyne *et al*, 1993; Doublié, 1997).

DNA fragments of human Par3 (residues 919–1028, 950–1022 and 919–950) were amplified from cDNA (Gene ID: 56288), and directly cloned into pGEX6P-3 using the BamHI and XhoI restriction enzyme sites. N-terminal GST-fused proteins were expressed in *E. coli* BL21-CodonPlus-RIL cells. The cells were disrupted by sonication at 4°C and the supernatant was applied onto a GST affinity column comprising glutathione sepharose 4B (GE Healthcare). After washing with 50 mM HEPES-Na (pH 7.5) buffer containing 150 mM NaCl and 1 mM dithiothreitol (DTT), fusion proteins were eluted with the same buffer containing 20 mM glutathione, 150 mM NaCl and 1 mM DTT. The GST-fused proteins were applied onto a Hitrap SP column and eluted with a NaCl concentration gradient (0.2–1.0 M).

Crystallization and data collection

$P6_222/P6_422$ crystals of the Tiam1 and $P4_122/P4_322$ crystals of the Tiam2 PH–CC–Ex regions were obtained as described earlier (Terawaki *et al*, 2008). $P2_1$ crystals of the Tiam1 PH–CC–Ex region were obtained within 2 weeks by mixing 1.0 μl of each reservoir solution, containing 20% PEG3350, 100 mM Tris–HCl (pH 8.5) and 200 mM $MgCl_2$, with 1.0 μl protein solution containing the PH–CC–Ex region and CD44 peptide (334–363) in a 1:3 molar ratio [0.5 mM Tiam2 PHCCEx and 1.5 mM CD44]. These crystals appeared to contain no CD44 peptide within the crystals. X-ray diffraction data of all crystals were collected using an ADSC quantum 315 CCD detector installed on the BL41XU beamline at SPring-8 from flash-cooled crystals using 25–30% (weight/volume) glycerol. All data were processed and scaled using the HKL2000 program (Otwinowski and Minor, 1997). The statistics are summarized in Table I.

Structural determination

Using data from the Tiam2 $P4_122/P4_322$ crystals, the positions of 19 selenium sites were determined using SHELX-D (Schneider and Sheldrick, 2002). Phasing and density modification were carried out using SHARP (Abrahams and Leslie, 1996) and SOLOMON (de la Fortelle and Bricogne, 1997), respectively. Model building was performed from the obtained electron density map using the graphic program COOT (Emsley and Cowtan, 2004). The structure was refined by the simulated annealing method using the program CNS (Brünger *et al*, 1998) to 3.2-Å resolution. The model was used for structural determination of the Tiam2 $P2_1$ crystal by the molecular replacement method using the program MOLREP (Vagin and Teplyakov, 1998). The structure was refined using CNS to 2.1-Å resolution (Table II). The crystal contains four Tiam2 PH–CC–Ex regions in the asymmetric units and the current structure includes 920 residues (232 residues of Mol_1, 231 of Mol_2, 229 of Mol_3 and 228 of Mol_4). No models were built for β3–β4 loop residues (6, 8, 9 and 12 residues for Mol_1, 2, 3 and 4, respectively), which were not observed in the electron density map. This analysis revealed no residual electron density that corresponded to the CD44 peptide. The Tiam1 PH–CC–Ex structure was determined by molecular replacement using MOLREP with the Tiam2 structure used as a search model. The structure was refined by the simulated annealing method using the program CNS to 4.5-Å resolution.

Peptide-binding studies

N-terminal biotinylated peptides were purchased from the Toray Research Center (Tokyo, Japan). The *in vitro* binding assay was carried out by the equilibrium SPR method using the Biacore Biosensor instrument (Biacore 3000; GE Healthcare). Peptides were coupled through the N-terminal biotin moiety to a streptavidin-coated sensor chip (SA sensor chip, Biacore AB). Purified PH–CC–Ex protein samples (0.001–100 μM) were injected into both peptide-linked and non-linked sensor chips for correction of background signals. All binding experiments were performed at 25°C with a flow rate of 5 μl/min in HBS-EP buffer comprising 10 mM HEPES (pH 7.4), 150 mM NaCl, 3 mM EDTA and 0.005% surfactant P20. For binding assay of human NMDAR, two peptides, the NMDAR loop I peptide consisting of residues 591–610 (VNSEEEEEDALTLS SAMWFS), which is located between transmembrane helices 1 and 2, and the NMDAR C-tail peptide consisting of residues 921–938 (AIEREEGQLQLCSRHRES) were used. The kinetic parameters were evaluated using the BIA evaluation software (GE Healthcare). The K_D values were obtained by the averaging of at least three independent measurements.

Pull-down assay

For each reaction, 30 μl of glutathione sepharose 4B resin (GE Healthcare) was mixed with 30 pmol of each N-terminal GST-fused Par3 fragment and suspended in 1 ml of 20 mM HEPES buffer (pH 7.5) containing 150 mM NaCl, 1 mM DTT (pull-down buffer) in a 1.5-ml tube (Eppendorf). The resin was harvested as a pellet by

Table I Crystallographic data

	Tiam2 Native I	Tiam2 Se-Met		Tiam2 Native II	Tiam1 Native
		Peak	Edge		
Data collection					
Space group	$P4_32_12$	$P4_32_12$	$P4_32_12$	$P2_1$	$P6_422$
Cell dimensions (Å)	$a=b=105.6$ $c=287.6$	$a=b=105.4$ $c=289.7$	$a=b=105.8$ $c=288.5$	$a=46.7$ $b=104.8$ $c=116.0$ $\beta=80.6$	$a=b=113.5$ $c=113.8$
Wavelength (Å)	1.0000	0.9789	0.9792	1.0000	1.0000
Resolution (Å)	50–3.2	50–3.4	50–3.4	50–2.08	50–4.5
Reflection					
Measured	336 843	540 236	503 703	23 4615	30 832
Unique	27 986	21 847	21 984	64 571	2824
Redundancy[a]	13.1 (9.5)	24.7 (16.1)	22.9 (13.7)	3.6 (2.9)	10.9 (8.3)
Completeness[a] (%)	91.7 (52.1)	93.6 (61.4)	94.3 (64.8)	97.6 (80.6)	98.7 (96.7)
Mean $I/\sigma(I)$[a]	38.8 (2.0)	41.3 (2.9)	34.6 (2.0)	20.0 (1.9)	13.8 (2.5)
R_{sym}[a] (%)	7.0 (66.1)	10.5 (51.3)	10.7 (55.6)	7.1 (50.2)	15.0 (68.2)
$R_{derivative}/R_{anomalous}$ (%)	23.8/6.2	24.3/4.8			
Phasing					
Heavy atom site		19			
R_{cullis} isomorphous (centric/acentric)		0.15/0.18	0.26/0.29		
Anomalous		0.73	0.92		
Phasing power isomorphous (centric/acentric)		2.60/2.44	0.97/1.04		
Anomalous		1.33	0.74		
Mean figure of merit centric/acentric		0.242/0.358			

[a]Each pair of values are for overall/outer shell.

Table II Structural refinements

	Tiam2 Native I	Tiam2 Native II	Tiam1
Refinement			
Resolution (Å)	50–3.2	30–2.1	50–4.5
R_{cryst}/R_{free} (%)	28.3/33.2	21.1/25.3	30.6/39.6
Number of residues			
Protein	924	920	230
Number of atoms			
Protein	7,416	7,371	1,143
Water	—	383	—
Mean B factor (Å^2)			
Total	144.5	39.1	107.0
Protein	—	39.0	—
Water	—	41.0	—
r.m.s deviation			
Bond lengths (Å)	0.008	0.006	0.009
Bond angles (deg)	1.172	1.111	1.717
Ramachandran plot			
Most favoured (%)	80.8	92.1	61.9
Additional allowed (%)	16.6	7.6	33.0
Generously allowed (%)	2.1	0.2	5.0
Disallowed (%)	0.5	0	0

centrifugation (2000 *g* for 2 min). After removing the supernatant, the resin was suspended in 1 ml of pull-down buffer containing 100 μM Tiam2 PH–CC–Ex and incubated overnight at 4°C with occasional mixing. The resin was then washed three times with pull-down buffer by centrifugation. To elute the GST-fused Par3 fragments and bound PH–CC–Ex, 30 μl of 20 mM HEPES buffer (pH 7.5) containing 150 mM NaCl, 1 mM DTT and 20 mM glutathione was added. After harvesting the resin as a pellet, fractions were mixed with 10 μl of SDS-sample buffer. The amount of GST-fused Par3 fragment and PH–CC–Ex protein in each eluted solution were determined using SDS–PAGE Stain (Invitrogen).

Coimmunoprecipitation

The cDNAs and the antibodies for the immunoblot analysis were obtained as described earlier (Nishimura *et al*, 2005). COS7 cells were grown in DMEM medium containing 10% fetal bovine serum.

For transfection, cells were seeded onto 100-mm dishes or 60-mm dishes. The plasmids were transfected in serum-free OptiMEM medium using Lipofetamine (Invitrogene), according to the manufacturer's instructions. The medium was exchanged to the fresh serum-containing medium after 4 h. After transfection, cells were incubated for 24 h at 37°C. For immunoprecipitation analysis, anti-GFP antibody and the protein-A beads (GE healthcare) were incubated with COS7 cell lysate transfected with the indicated plasmids (coding GFP-Par3 and the wild type or mutant HA-Tiam1) in lysis buffer (20 mM Tris–HCl pH 7.5, 100 mM NaCl, 1 mM EDTA, 1 mM DTT, 1% NP-40) for 1 h at 4°C. The beads were washed three times with lysis buffer, and the washed beads were suspended with SDS–PAGE sampling buffer. The bound proteins were subjected to immunoblot analysis.

Cell morphology assay

Quantitative analysis of the inhibitory effects of the isolated Tiam1 PHCCEx domain on lamellipodia formation was performed as described earlier (Nishimura *et al*, 2005). COS7 cells were transfected with plasmids coding the myc-tagged Par3 4N/1 fragment and the GFP-tagged Tiam1 PHCCEx domain. The Par-3 4N/1 fragment encompassing the Tiam1/2-binding region (residues 937–1038) that is sufficient to increase the amount of Rac1-GTP for induction of lamellipodia by binding to Tiam1 (Nishimura *et al*, 2005). The isolated wild-type Tiam1 PHCCEx domain was known to be a dominant-negative factor that interferes with Par-3-Tiam1 binding (Matsuo *et al*, 2002; Nishimura *et al*, 2005). Inhibition of the Par-3 4N/1-mediated lamellipodia formation by the wild-type and mutant Tiam1 PHCCEx domains was estimated with the GFP-positive cells scored by the presence of lamellipodia. Data are means ± s.d. of three independent experiments.

Accession codes

Protein Data Bank: Coordinates and structure factors for the Tiam1 and Tiam2 PHCCEx domains have been deposited (accession codes 3A8N, 3A8P and 3A8Q).

Supplementary data

Supplementary data are available at *The EMBO Journal* Online (http://www.embojournal.org).

Acknowledgements

This work was supported by a Grant-in-Aid for Scientific Research (A) and Scientific Research on Priority Areas, Cancer and Macromolecular assembly structure from the Ministry of Education, Culture, Sports, Science and Technology (MEXT) of Japan (to TH), a research grant from the Uehara Memorial Foundation and the Foundation for NAIST (to TH). We thank the beamline staff of BL41XU of SPring-8 at Harima for help with the data collection. ST and TM are recipients of a postdoctoral fellowship from the 21st Century COE Program and the Global COE Program in NAIST from MEXT of Japan, respectively.

Conflict of interest

The authors declare that they have no conflict of interest.

References

Abrahams JP, Leslie AG (1996) Methods used in the structure determination of bovine mitochondrial F1 ATPase. *Acta Crystallogr D Biol Crystallogr* **52:** 30–42

Adithi M, Venkatesan N, Kandalam M, Biswas J, Krishnakumar S (2006) Expressions of Rac1, Tiam1 and Cdc42 in retinoblastoma. *Exp Eye Res* **83:** 1446–1452

Bourguignon LY, Zhu H, Shao L, Chen YW (2000) CD44 interaction with tiam1 promotes Rac1 signaling and hyaluronic acid-mediated breast tumor cell migration. *J Biol Chem* **275:** 1829–1838

Brünger AT, Adams PD, Clore GM, DeLano WL, Gros P, Grosse-Kunstleve RW, Jiang JS, Kuszewski J, Nilges M, Pannu NS, Read RJ, Rice LM, Simonson T, Warren GL (1998) Crystallography & NMR system: a new software suite for macromolecular structure determination. *Acta Crystallogr D Biol Crystallogr* **54:** 905–921

Buchsbaum RJ, Connolly BA, Feig LA (2002) Interaction of Rac exchange factors Tiam1 and Ras-GRF1 with a scaffold for the p38 mitogen-activated protein kinase cascade. *Mol Cell Biol* **22:** 4073–4085

Buchsbaum RJ, Connolly BA, Feig LA (2003) Regulation of p70 S6 kinase by complex formation between the Rac guanine nucleotide exchange factor (Rac-GEF) Tiam1 and the scaffold spinophilin. *J Biol Chem* **278:** 18833–18841

Burks DJ, Wang J, Towery H, Ishibashi O, Lowe D, Riedel H, White MF (1998) IRS pleckstrin homology domains bind to acidic motifs in proteins. *J Biol Chem* **273:** 31061–31067

Ceccarelli DFJ, Blasutig IM, Goudreault M, Li Z, Ruston J, Pawson T, Sicheri F (2007) Non-canonical interaction of phosphoinositides with pleckstrin homology domains of Tiam1 and ArhGAP9. *J Biol Chem* **282:** 13864–13874

Chen X, Macara IG (2005) Par-3 controls tight junction assembly through the Rac exchange factor Tiam1. *Nat Cell Biol* **7:** 262–269

Connolly BA, Rice J, Feig LA, Buchsbaum RJ (2005) Tiam1-IRSp53 complex formation directs specificity of rac-mediated actin cytoskeleton regulation. *Mol Cell Biol* **25:** 4602–4614

DiNitto JP, Lambright DG (2006) Membrane and juxtamembrane targeting by PH and PTB domains. *Biochim Biophys Acta* **1761:** 850–867

Doublié S (1997) Preparation of selenomethionyl proteins for phase determination. *Methods Enzymol* **276:** 523–530

Duyne GDV, Standaert RF, Karplus PA, Schreiber SL, Clardy J (1993) Atomic structures of the human immunophilin FKBP-12 complexes with FK506 and rapamycin. *J Mol Biol* **229:** 105–124

Emsley P, Cowtan K (2004) Coot: model-building tools for molecular graphics. *Acta Crystallogr D Biol Crystallogr* **60:** 2126–2132

Engers R, Zwaka TP, Gohr L, Weber A, Gerharz CD, Gabbert HE (2000) Tiam1 mutations in human renal-cell carcinomas. *Int J Cancer* **88:** 369–376

de la Fortelle E, Bricogne G (1997) Maximum-likelihood heavy-atom parameter refinement for multiple isomorphous replacement and multiwavelength anomalous diffraction methods. *Methods Enzymol* **276:** 472–494

Godi A, Campli AD, Konstantakopoulos A, Tullio GD, Alessi DR, Kular GS, Daniele T, Marra P, Lucocq JM, Matteis MAD (2004) FAPPs control Golgi-to-cell-surface membrane traffic by binding to ARF and PtdIns(4)P. *Nat Cell Biol* **6:** 393–404

Habets GG, Scholtes EH, Zuydgeest D, van der Kammen RA, Stam JC, Berns A, Collard JG (1994) Identification of an invasion-inducing gene, Tiam-1, that encodes a protein with homology to GDP-GTP exchangers for Rho-like proteins. *Cell* **77:** 537–549

Hakoshima T, Shimizu T, Maesaki R (2003) Structural basis of the Rho GTPase signaling. *J Biochem* **134:** 327–331

Hamada K, Shimizu T, Matsui T, Tsukita SH, Tsukita SA, Hakoshima T (2000) Structural basis of the membrane-targeting and unmasking mechanisms of the radixin FERM domain. *EMBO J* **19:** 4449–4462

Hamada K, Shimizu T, Yonemura S, Tsukita SH, Tsukita SA, Hakoshima T (2003) Structural basis of adhesion-molecule recognition by ERM proteins revealed by the crystal structure of the radixin-ICAM-2 complex. *EMBO J* **22:** 502–514

Hoshino M, Sone M, Fukata M, Kuroda S, Kaibuchi K, Nabeshima Y, Hama C (1999) Identification of the stef gene that encodes a novel guanine nucleotide exchange factor specific for Rac1. *J Biol Chem* **274:** 17837–17844

Hyvönen M, Macias MJ, Nilges M, Oschkinat H, Saraste M, Wilmanns M (1995) Structure of the binding site for inositol phosphates in a PH domain. *EMBO J* **14:** 4676–4685

Lemmon MA (2008) Membrane recognition by phospholipid-binding domains. *Nat Rev Mol Cell Biol* **9:** 99–111

Levine TP, Munro S (2002) Targeting of Golgi-specific pleckstrin homology domains involves both PtdIns 4-kinase-dependent and -independent components. *Curr Biol* **12:** 695–704

Liu L, Wu D, Ding Y (2005) Tiam1 gene expression and its significance in colorectal carcinoma. *World J Gastroenterol* **11:** 705–707

Liu L, Zhao L, Zhang Y, Zhang Q, Ding Y (2007) Proteomic analysis of Tiam1-mediated metastasis in colorectal cancer. *Cell Biol Int* **31:** 805–814

Malliri A, van der Kammen RA, Clark K, van der Valk M, Michiels F, Collard JG (2002) Mice deficient in the Rac activator Tiam1 are resistant to Ras-induced skin tumours. *Nature* **417:** 867–871

Malliri A, Rygiel TP, van der Kammen RA, Song J, Engers R, Hurlstone AFL, Clevers H, Collard JG (2006) The rac activator Tiam1 is a Wnt-responsive gene that modifies intestinal tumor development. *J Biol Chem* **281:** 543–548

Marinissen MJ, Gutkind JS (2005) Scaffold proteins dictate Rho GTPase-signaling specificity. *Trends Biochem Sci* **30:** 423–426

Matsuo N, Hoshino M, Yoshizawa M, Nabeshima Y (2002) Characterization of STEF, a guanine nucleotide exchanger factor for Rac1, required for neurite growth. *J Biol Chem* **277:** 2860–2868

Mertens AE, Roovers RC, Collard JG (2003) Regulation of Tiam1-Rac signalling. *FEBS Lett* **546:** 11–16

Michiels F, Habets GG, Stam JC, van der Kammen RA, Collard JG (1995) A role for Rac in Tiam1-induced membrane ruffling and invasion. *Nature* **375:** 338–340

Michiels F, Stam JC, Hordijk PL, van der Kammen RA, Stalle LR, Feltkamp CA, Collard JG (1997) Regulated membrane localization of Tiam1, mediated by the NH2-terminal pleckstrin homology domain, is required for Rac-dependent membrane ruffling and C-Jun NH2-terminal kinase activation. *J Cell Biol* **137:** 387–398

Minard ME, Kim L, Price JE, Gallick GE (2004) The role of the guanine nucleotide exchange factor Tiam1 in cellular migration, invasion, adhesion and tumor progression. *Breast Cancer Res Treat* **84:** 21–32

Mori T, Kitano K, Terawaki S, Maesaki R, Fukami Y, Hakoshima T (2008) Structural basis for CD44 recognition by ERM proteins. *J Biol Chem* **283:** 29602–29612

Murzin AG, Brenner SE, Hubbard T, Chothia C (1995) SCOP: a structural classification of proteins database for the investigation of sequences and structures. *J Mol Biol* **247:** 536–540

Nishimura T, Yamaguchi T, Kato K, Yoshizawa M, Nabeshima Y, Ohno S, Hoshino M, Kaibuchi K (2005) PAR-6-PAR-3 mediates Cdc42-induced Rac activation through the Rac GEFs STEF/Tiam1. *Nat Cell Biol* **7:** 270–277

Otwinowski Z, Minor W (1997) Processing of X-ray diffraction data collected in oscillation mode. *Methods Enzymol* **276:** 307–326

Prehoda KE, Lee DJ, Lim WA (1999) Structure of the enabled/VASP homology 1 domain-peptide complex: a key component in the spatial control of actin assembly. *Cell* **97:** 471–480

Rameh L, Arvidsson A, Carraway K, Couvillon A, Rathbun G, Crompton A, VanRenterghem B, Czech M, Ravichandran K, Burakoff S, Wang D, Chen C, Cantley LA (1997) Comparative analysis of the phosphoinositide binding specificity of pleckstrin homology domains. *J Biol Chem* **272:** 22059–22066

Ritter B, Denisov AY, Philie J, Allaire PD, Legendre-Guillemin V, Zylbergold P, Gehring K, McPherson PS (2007) The NECAP PHear domain increases clathrin accessory protein binding potential. *EMBO J* **26:** 4066–4077

Rossman KL, Der CJ, Sondek J (2005) GEF means go: turning on RHO GTPases with guanine nucleotide-exchange factors. *Nat Rev Mol Cell Biol* **6:** 167–180

Schneider TR, Sheldrick GM (2002) Substructure solution with SHELXD. *Acta Crystallogr D Biol Crystallogr* **58:** 1772–1779

Sone M, Hoshino M, Suzuki E, Kuroda S, Kaibuchi K, Nakagoshi H, Saigo K, Nabeshima Y, Hama C (1997) Still life, a protein in synaptic terminals of Drosophila homologous to GDP-GTP exchangers. *Science* **275:** 543–547

Stam JC, Sander EE, Michiels F, van Leeuwen FN, Kain HE, van der Kammen RA, Collard JG (1997) Targeting of Tiam1 to the plasma membrane requires the cooperative function of the N-terminal pleckstrin homology domain and an adjacent protein interaction domain. *J Biol Chem* **272:** 28447–28454

Takai Y, Kitano K, Terawaki S, Maesaki R, Hakoshima T (2007) Structural basis of PSGL-1 binding to ERM proteins. *Genes Cells* **12:** 1329–1338

Takai Y, Kitano K, Terawaki S, Maesaki R, Hakoshima T (2008) Structural basis of the cytoplasmic tail of adhesion molecule CD43 and its binding to ERM proteins. *J Mol Biol* **381:** 634–644

Tanaka M, Ohashi R, Nakamura R, Shinmura K, Kamo T, Sakai R, Sugimura H (2004) Tiam1 mediates neurite outgrowth induced by ephrin-B1 and EphA2. *EMBO J* **23:** 1075–1088

Terawaki S, Kitano K, Hakoshima T (2007) Structural basis for type II membrane protein binding by ERM proteins revealed by the radixin-neutral endopeptidase 24.11 (NEP) complex. *J Biol Chem* **282:** 19854–19861

Terawaki S, Kitano K, Hakoshima T (2008) Crystallographic characterization of the membrane-targeting domains of the Rac-specific guanine nucleotide-exchange factors Tiam1 and Tiam2. *Acta Crystallogr F Struct Biol Cryst Commun* **64:** 1039–1042

Tolias KF, BiKoff JB, Burette A, Paradis S, Harrar D, Tavazoie S, Weinberg RJ, Greenberg ME (2005) The Rac1-GEF Tiam1 couples the NMDA receptor to the activity-dependent development of dendritic arbors and spines. *Neuron* **45:** 525–538

Tolias KF, Bikoff JB, Kane CG, Tolias CS, Hu L, Greenberg ME (2007) The Rac1 guanine nucleotide exchange factor Tiam1 mediates EphB receptor-dependent dendritic spine development. *Proc Natl Acad Sci USA* **104:** 7265–7270

Vagin A, Teplyakov A (1998) A translation-function approach for heavy-atom location in macromolecular crystallography. *Acta Crystallogr D Biol Crystallogr* **54:** 400–402

Vetter IR, Nowak C, Nishimoto T, Kuhlmann J, Wittinghofer A (1999) Structure of a Ran-binding domain complexed with Ran bound to a GTP analogue: implications for nuclear transport. *Nature* **398:** 39–46

Worthylake DK, Rossman KL, Sondek J (2000) Crystal structure of Rac1 in complex with the guanine nucleotide exchange region of Tiam1. *Nature* **408:** 682–688

Yonemura S, Hirao M, Doi Y, Takahashi N, Kondo T, Tsukita SA, Tsukita SH (1998) Ezrin/radixin/moesin (ERM) proteins bind to a positively charged amino acid cluster in the juxta-membrane cytoplasmic domain of CD44, CD43, and ICAM-2. *J Cell Biol* **140:** 885–895

Zhao C, Du G, Skowronek K, Frohman MA, Bar-Sagi D (2007) Phospholipase D2-generated phosphatidic acid couples EGFR stimulation to Ras activation by Sos. *Nat Cell Biol* **9:** 706–712

